

Jinsong YU  
Jie YANG  
Diyin TANG  
Jing DAI

## EARLY PREDICTION OF REMAINING DISCHARGE TIME FOR LITHIUM-ION BATTERIES CONSIDERING PARAMETER CORRELATION BETWEEN DISCHARGE STAGES

### WCZESNE PRZEWIDYWANIE CZASU POZOSTAŁEGO DO ROZŁADOWANIA BATERII LITOWO-JONOWEJ Z UWZGLĘDNIENIEM KORELACJI PARAMETRÓW Z RÓŻNYCH ETAPÓW PROCESU ROZŁADOWANIA

*In this paper, we propose a method for making early predictions of remaining discharge time (RDT) that considers information about future battery discharge process. Instead of analyzing the entire degradation process of a battery, as in the existing literature, we obtain the information about future battery condition by decomposing the discharge model into three stages, according to level of voltage loss. Correlation between model parameters at the first and last stages of discharge process allows the values of model parameters in the future to be used to predict the value of parameters at early stages of discharge. The particle swarm optimization (PSO) and particle filter (PF) algorithms are employed to update parameters when new voltage data is available. A case study demonstrates that the proposed approach predicts RDT more accurately than the benchmark PF-based prediction method, regardless of the degradation period of the battery.*

**Keywords:** *Lithium-ion battery, parameter correlation, particle swarm optimization, particle filter, remaining discharge time prognostics.*

*W pracy zaproponowano metodę wczesnego przewidywania czasu pozostałego do rozładowania baterii (RDT), która uwzględni informacje na temat przyszłego procesu jej rozładowywania. Zamiast analizować cały proces degradacji baterii, jak to ma miejsce w literaturze przedmiotu, wykorzystano informacje o przyszłym stanie baterii uzyskane na drodze podziału modelu procesu rozładowania na trzy etapy, według poziomu utraty napięcia. Korelacje między parametrami modelu uzyskanymi na pierwszym i ostatnim etapie procesu rozładowania baterii umożliwiają wykorzystanie przyszłych wartości parametrów do przewidywania wartości parametrów we wczesnych etapach rozładowania. Do aktualizacji parametrów zgodnie z naphywającymi nowymi danymi napięciowymi wykorzystano algorytm optymalizacji rojem cząstek (PSO) i algorytm filtra cząsteczkowego (PF). Studium przypadku pokazuje, że proponowane podejście pozwala bardziej precyzyjnie prognozować RDT niż metoda prognozowania oparta na PF, niezależnie od okresu degradacji baterii.*

**Słowa kluczowe:** *bateria litowo-jonowa, korelacja parametrów, optymalizacja rojem cząstek, filtr cząsteczkowy, prognozowanie czasu do rozładowania.*

#### 1. Introduction

The lithium-ion battery is a popular power source and is commonly used in a range of applications such as portable electronic devices and electric vehicles. Compared with other widely used energy sources, the lithium-ion battery possesses high energy density, high power density, long service life, and is environmentally friendly [14]. Early prediction of remaining discharge time (RDT) is crucial to battery health management and system stability. If a battery runs out without timely charging, it is harmful to battery health and longevity and can sometimes lead to system failure, or even precipitate a disaster.

In most previous studies of RDT prediction, methods have utilized state-of-charge (SOC) and state-of-energy (SOE) as the indicators that announce the end of discharge, e.g., [6,32,12,28,11]. When the SOC or the SOE of a battery reaches a certain level, the battery is considered to have run out of power. In these methods, accurate values for SOC and SOE are of vital importance in RDT prediction.

However, for most real applications, accurate estimation of SOC or SOE is difficult, for they are indirectly measured and require the introduction of additional relevant variables for estimation [17]. Therefore, some research has resorted to using more easily measured variables in RDT prediction, such as battery output voltage. Saha et al. [20, 22] and Dalal et al. [4] used battery output voltage to predict RDT in a lumped parameter battery model with particle filter, and Orchard et al. [16] used it in an empirical state-space model with sequential Monte Carlo.

After indicators are selected, the usual way of predicting RDT in existing literature is through a physical model and a filtering-based method that updates the model parameters when observations become available. Particle filtering (PF) is a commonly used filtering-based method. PF is an entirely nonlinear state estimator based on probability that can be used to update battery model states and parameters based on new voltage data [34,15]. However, although PF can provide

an accurate characterization of uncertainty in the filtering stage, it is very sensitive to the initial conditions of the state-space model and does poorly in long-term prediction, especially when uncertain initial conditions related to usage, and age or battery degradation progress exist [18]. Therefore, measures that avoid or alleviate dependence on initial states are a consideration in PF-based prediction methods.

Examples of such measures in the literature are radial basis function neural network [23], relevance vector regression [33], recursive least-square-algorithm method [5], and expectation-maximum method [29]. These methods are used in combination with PF-based methods in RDT prediction. They are effective to some extent because they better exploit all available information in adaptive updating but they only consider current and historical battery information. If future information about battery discharge could be incorporated, knowledge about the future values of model parameters would enable more reliable predictions, especially at the early stage of the discharge. Information about future battery degradation is one example of data that could improve RDT prediction for it allows examination of battery characteristics over the whole lifecycle as a factor influencing the discharge process. Liu et.al [13] employed data-driven method to learn systems degradation patterns so as to predict future measurements, and these predicted measurements are incorporated into PF update the parameters of model. Wang et.al [27] proposed a capacity prognostics method consisting of RVM and a conditional three-parameter capacity degradation model. RVM was used to obtain the most representative relevant vectors and to determine the parameters of the capacity degradation model. Xu et al. [30] proposed a hierarchical model that included a comprehensive consideration of both the discharge process and degradation process for predicting RDT in different cycles. Yu et al. [31] described different voltage trajectory patterns using a Dirichlet process mixture model that considered different periods in the lifetime of a battery.

In this paper, we consider information about future battery discharge process in achieving an early prediction of RDT. Early prediction of RDT is important because it provides vital information that could enable electric machines and vehicles to organize operation tasks and avoid power run-out emergencies. Instead of analyzing the whole degradation process of a battery, as in existing studies, we derive information about future battery discharge by decomposing the discharge model into three stages according to voltage loss. Correlations between the values of model parameters at first and last stages of discharge provide us with knowledge about the values of parameters in the future, allowing us to better estimate model parameters at early stages of discharge. To combine the observations in prediction, we use particle swarm optimization (PSO) and particle filter (PF) to update model parameters when new observations of voltage data become available. In a case study employing real data, we demonstrate that our proposed method predicts RDT more accurately than benchmark PF-based methods, regardless of the degradation period of the battery.

The rest of the paper is structured as follows. Section 2 introduces the discharge model. Section 3 develops the quantitative correlation between parameters. Section 4 describes RDT Prediction using the PSO and PF methods with age-related parameters correlation between discharge stages. The results and analysis of the case study are presented in section 5. Conclusions are presented in section 6.

## 2. Battery Model

### 2.1. Description of the individual discharge process

As a battery discharge progresses, its voltage will decrease over time until it hits a threshold. The electrochemical model can be used to describe the voltage trajectory [25, 3, 9]. However, it is difficult and usually time consuming to build an accurate model of the battery discharge process because of the complexity of the electrochemical

reaction. Therefore, this paper adopts the empirical model proposed by Saha and Goebel [20]. The critical advantage of empirical models is their flexible and simple structure. Although the empirical model is only based on the analysis of experimental data and does not consider the electrochemical reaction process, the parameters in our model describe real physical characteristics of batteries. Empirical models are also easy to establish, compared to other models. Our proposed model consists of several parts representing different levels of voltage loss in the discharge process, as shown below:

$$E(t) = E_0 - \Delta E_{sd}(t) - \Delta E_{mt}(t) - \Delta E_{rd}(t) \quad (1)$$

where  $t$  is the time variable during the discharge process,  $E_0$  is the Gibbs free energy, i.e. the theoretical output potential for the given chemistry, and can also be regarded as the terminal voltage with full charged,  $\Delta E_{sd}(t)$  is the voltage loss of self-discharge,  $\Delta E_{mt}(t)$  is the voltage loss of internal resistance to mass transfer, and  $\Delta E_{rd}(t)$  is the voltage loss of cell reactant depletion. The several parts can be represented as:

$$\Delta E_{sd}(t) = a_1 e^{-\frac{a_2}{t}} \quad (2)$$

$$\Delta E_{mt}(t) = \Delta E_{init} - a_5 t \quad (3)$$

$$\Delta E_{rd}(t) = a_3 e^{a_4 t} \quad (4)$$

where  $\Delta E_{init}$  is the initial voltage drop. This model can also be represented by:

$$E(t) = E'_0 - a_1 e^{-\frac{a_2}{t}} - a_3 e^{a_4 t} + a_5 t \quad (5)$$

where  $E'_0 = E_0 - \Delta E_{init}$ ,  $E'_0$  is the initial voltage value. The model has 5 parameters  $\{a_1, a_2, a_3, a_4, a_5\}$ ,  $a_1, a_2$  are related to self-discharge,  $a_3, a_4$  are related to cell reactant depletion, and  $a_5$  is related to internal resistance to mass transfer. Fig. 1 shows the different voltage loss levels in a single discharge. In Fig. 1,  $E_1(t) = E'_0 - \Delta E_{sd}(t)$ ,  $E_2(t) = E_0 - \Delta E_{mt}(t)$ ,  $E_3(t) = E'_0 - \Delta E_{rd}(t)$ . As we can see in Fig. 1, the discharge process consists of three stages related to the above three levels. In the first stage, the voltage decreases rapidly because of self-discharge. In the second stage, the decline is at a constant rate for a long time due to internal resistance to mass transfer. In the third stage, voltage has fallen dramatically because of cell reactant depletion. In the rest of this paper, we use the terms “self-discharge stage”,

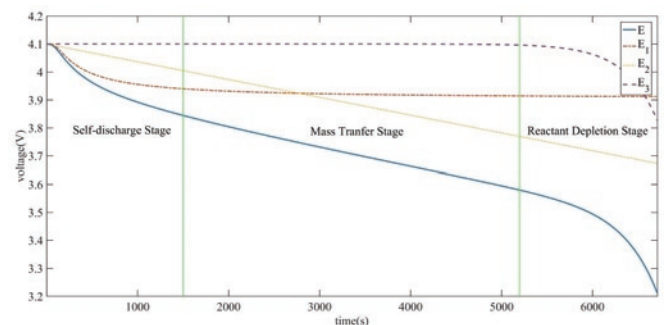


Fig. 1. Decomposition of Li-ion discharge process into different voltage loss levels

“mass transfer stage”, and “reactant depletion stage”, respectively, when referring to the above three stages. Note that  $E_1$  is decreasing in first stage only and remains unchanged later, while  $E_3$  is decreasing in the third stage only and remains unchanged earlier. So,  $\Delta E_{sd}(t)$  plays a leading role in the first stage and  $\Delta E_{rd}(t)$  plays a leading role in the third stage.

### 2.2. Description of battery degradation

We present a case study of Li-ion batteries to demonstrate the performance of our proposed method for battery RDT prediction. We used the 18650 Li-ion batteries data set provided by NASA Ames Research Center for illustration [2]. A set of four 18650 Li-ion batteries were continuously operated by repeatedly charging them to 4.2V and then discharging them to 3.2V using a randomized sequence of discharging currents between 0.5A and 4A. The sequence of discharging currents in the discharge process mimicked randomized use in real practice. Here, this type of discharging profile is referred to as random walk (RW) discharging. In this paper, we tested three 18650 Li-ion batteries identified as RW3, RW4, and RW5 and extracted overall reference cycles and numbered them from the 1st cycle, for convenience. Reference charging and discharging cycles were performed twice after every fifty random walk cycles. In charging cycles, batteries are first charged at 2A (constant current), until they reach 4.2V, at which time the charging switches to a constant voltage mode and continues charging the batteries until the charging current falls below 0.01A. And in discharging cycles, batteries are then discharged at 2A until the battery voltage crosses 3.2V. Fig. 2 shows all reference discharging cycles for RW3. One can see that the third stage of all discharge process is moving left as battery ages, while the first stage is moving down as battery ages. And, we can see that the third stage is dynamic and changes rapidly, making RDT prediction difficult.

However, we have already seen that  $\Delta E_{sd}(t)$  plays a leading role in the first stage and  $\Delta E_{rd}(t)$  plays a leading role in the third stage. Therefore, we can assume that  $\Delta E_{rd}(t)$  and  $\Delta E_{sd}(t)$  parameters have a known aging trend, we can specify the quantitative relationship between them. If we can use the relationship between a parameter in  $\Delta E_{rd}(t)$  and a parameter in  $\Delta E_{sd}(t)$ , then the prediction of RDT will be more accurate. In the prediction of RDT, we can often get an accurate  $a_1$  early but  $a_4$  is unknown initially. To build the relationship between the first and the last stages, we assumed that only one parameter in  $\Delta E_{rd}(t)$  and  $\Delta E_{sd}(t)$  cause the decrease of voltage. Considering parameter orders of magnitude and the main factors in voltage drops, we chose  $a_1$  in  $\Delta E_{sd}(t)$  and  $a_4$  in  $\Delta E_{rd}(t)$ . In testing, we found that  $a_1$  and  $a_4$  have a linear relationship. We propose an approach to identify the parameters and define this linear relation in the following section.

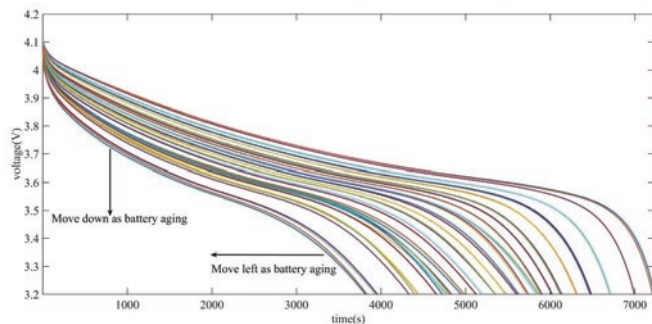


Fig.2. All reference discharge cycles in RW3

In conclusion, an individual discharge profile includes three stages, i.e. the self-discharge stage, the mass transfer stage and the reactant depletion stage. Our empirical model includes three parts representing the different levels of voltage loss related to the three stages

above. When information from the third stage is not available, we can't obtain accurate parameters.

From the perspective of group discharge profiles in the whole life of a battery, the third stage of all discharge profiles is moving left as battery ages, while the first stage is moving down as battery ages. So, we can use age-related parameters to describe battery degradation. The third stage is dynamic and changes rapidly, making RDT prediction difficult. The quantitative relationship between age-related parameters in the first and third stages makes it possible to predict RDT in early stages of the discharge process.

## 3. Modeling procedure

### 3.1. Parameter identification

Particle swarm optimisation (PSO) is a global random search algorithm based on swarm intelligence, proposed by Kennedy and Eberhart in 1995 [10]. PSO is widely used in nonlinear parameter identification [24, 19, 8] because the approach is simple, efficient, easy to implement, and has fewer parameters to adapt. In this study, we used Particle Swarm Optimization for parameter identification to obtain all parameter degradation trends. In PSO, each particle remembers the optimal solution for itself and the whole swarm and moves toward the global optimal solution. At the same time, particles share information with each other. PSO's equations are shown below:

$$v_{p,d}(t) = wv_{p,d}(t-1) + c_1r_1(p_{p,d}^{ind} - x_{p,d}(t-1)) + c_2r_2(p_d^{glo} - x_{p,d}(t-1)) \quad (6)$$

$$x_{p,d}(t) = x_{p,d}(t-1) + v_{p,d}(t) \quad (7)$$

where  $p$  is the particle,  $d$  is the search direction, and  $t$  is the iteration number;  $p^{ind}$  is the best solution for the particle itself while  $p^{glo}$  is the optimal solution for the whole swarm;  $x_{p,d}$  is the position of a particle and  $v_{p,d}$  is the velocity of the particle;  $w$ ,  $c_1$ ,  $c_2$  are the search parameters of PSO;  $r_1$  and  $r_2$  are uniform random numbers within the range of 0 and 1. In Equation (6), the first term represents inertia and demonstrates that particles tend to maintain prior velocity. The second term describes cognition and shows that a particle is inclined to move toward the optimal solution for itself. The last term represents the social behavior of particles in PSO and describes how particles have a tendency to arrive at the optimal solution for the whole swarm.

A crucial component of PSO methods is the fitness function, or the objection function, and here we choose the root mean squared error (RMSE) as the fitness function, expressed as:

$$RMSE = \sqrt{\frac{1}{N} \sum_{i=1}^N (V_i(t) - E_i(t))^2} \quad (8)$$

where  $t$  is the time variable,  $N$  is the number of data points,  $V$  is the measured experimental voltage output, and  $E$  is the model's voltage output.

In the test below, we use RW3, RW4, RW5 to extract all the reference discharge cycles in the entire battery life cycle. We apply PSO to identify the parameters of the model and to find all the parameter depletion trends. Figs. 3-5 display the results of the parameters ageing trends as the number of cycles increases. We can see from the graphs that parameters  $a_1$  and  $a_4$  have the same linear aging trend, indicating that they may be related. In the next, we attempt to define the relationship between them.

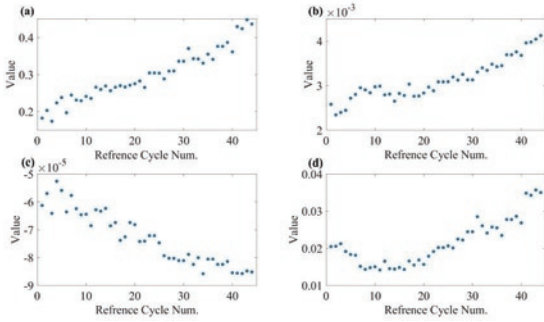


Fig. 3. RW3 parameters aging trend of (a)  $a_1$ , (b)  $a_4$ , (c)  $a_5$ , and (d) RMSE

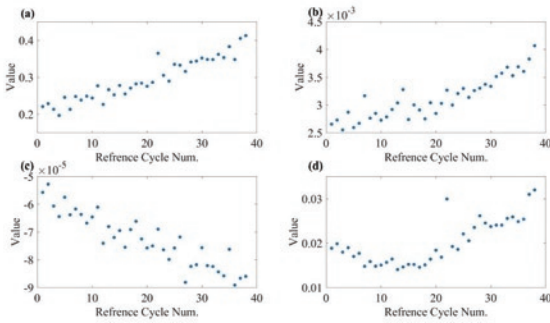


Fig. 4. RW4 parameters aging trend of (a)  $a_1$ , (b)  $a_4$ , (c)  $a_5$ , and (d) RMSE

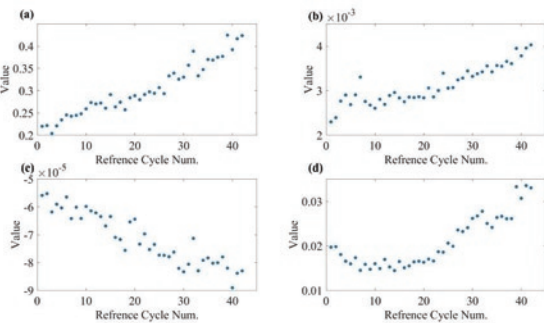


Fig. 5. RW5 parameters aging trend of (a)  $a_1$ , (b)  $a_4$ , (c)  $a_5$ , and (d) RMSE

Table 1. The linear relationship between  $a_1$  and  $a_4$

Battery Coefficient	RW3	RW4	RW5
$m_1$	0.006122	0.005816	0.006470
$m_2$	0.001584	0.001708	0.001182

### 3.2. Age-related parameters correlation between stages

Here, we use the least squares method to describe the linear relationship between  $a_1$  and  $a_4$ . Fig. 6 shows curve fitting for RW3, RW4, RW5. We see a high degree of linear correlation between  $a_1$  and  $a_4$ . This linear relationship between  $a_1$  and  $a_4$  can be expressed as:

$$a_4 = m_1 a_1 + m_2 \tag{9}$$

where  $m_1$  and  $m_2$  are the coefficients of the linear equation. The estimation of coefficients for Equation 9 are shown in Table 1. As we saw in Fig. 2, the third stage of the discharge process is dynamic and changes rapidly, increasing the difficulty of arriving at a prognosis for battery RDT. While in the early prediction there is no information about  $a_4$  prior to RDT prediction, the value of  $a_4$  will directly impacts RDT prediction accuracy. Therefore, once having specified the relationship between  $a_1$  and  $a_4$  using historical data, we can obtain a more accurate parameter  $a_4$  for use in early prediction.

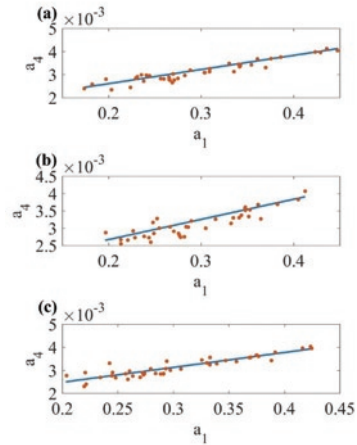


Fig. 6.  $a_1$  and  $a_4$  linear relationship results of (a) RW3, (b) RW4, (c) RW5

## 4. RDT Prediction

### 4.1. Revising parameters in process with the PSO Method

In this section, we describe how parameters are revised in PSO for new discharge cycles. As mentioned previously, in this model, we suppose that  $a_2$  and  $a_3$  remain fixed. Due to the relationship between  $a_1$  and  $a_4$ , we can derive  $a_4$  when the value of  $a_1$  is given. Therefore, we only need to update the parameter values,  $a_1, a_5$ . From the section 2,  $\Delta E_{rd}(t) = a_3 e^{a_4 t}$ , or very nearly zero, so our model can be expressed as:

$$E(t) = E'_0 - a_1 e^{-\frac{a_2}{t}} + a_5 t \tag{10}$$

Parameter identification with PSO was introduced in section 3. The fitness function used here is the same as described in that section. Using the PSO method, we obtain approximate values of the parameters that will be updated after new discharge cycles complete. PF is used to update the parameters and make the RDT prediction.

### 4.2. RDT Prediction via the Particle Filtering Method

Particle filtering is an effective method in battery RDT prediction, considered more accurate than other methods. Walker et al. [26] showed that PF is more precise than non-linear least squares (NLLS) and the unscented Kalman filter (UKF) for predicting the RDT of a lithium-ion battery. The PF is a non-linear filter, combining a Bayesian learning method with important sampling to obtain a good state for tracking performance online.

We use the PF framework for RDT prediction in our proposed method. We consider the model coefficients  $\{a_1, a_2, a_3, a_4, a_5\}$  as the state variables in the state transition model. Using the PSO method,

we obtain the initial parameters  $\{a_1, a_4, a_5\}$ , in which  $a_4 = m_1 a_1 + m_2$ . So, the system transition and measurement functions can be written as: State transition model:

$$a_{1,i+1} = a_{1,i} + \omega_{1,i} \quad (11)$$

$$a_{2,i+1} = a_{2,i} + \omega_{2,i} \quad (12)$$

$$a_{3,i+1} = a_{3,i} + \omega_{3,i} \quad (13)$$

$$a_{4,i+1} = a_{4,i} + \omega_{4,i} \quad (14)$$

$$a_{5,i+1} = a_{5,i} + \omega_{5,i} \quad (15)$$

Measurement model:

$$E_i = E'_0 - a_{1,i+1} e^{-\frac{a_{2,i+1}}{t}} - a_{3,i+1} e^{a_{4,i+1}t} + a_{5,i+1}t + \bar{v}_i \quad (16)$$

where  $\omega_{1,i}, \omega_{2,i}, \omega_{3,i}, \omega_{4,i}, \omega_{5,i}$  are process noise and have a zero-mean Gaussian distribution;  $v_i$  is the measurement noise, which also follows a zero-mean Gaussian distribution;  $m_1, m_2$  are the coefficients of the linear relationship between  $a_1$  and  $a_4$ . With given less data, we can use the linear relationship between  $a_1$  and  $a_4$  to derive the parameter  $a_4$  from  $a_1$ .

PF, as a sequential Monte Carlo method, implements a recursive Bayesian filter by simulation-based methods [7]. In PF, many particles are generated, all particles weights are updated based on new observations, and the posterior density function (PDF) of the set of particles is derived. To consider the evolution of the state sequence  $\{x_k, k \in \mathbb{N}\}$ , and the set of all available measurements  $z_{1:k} = \{z_i, i = 1, 2, \dots, k\}$  up to time  $k$ , PDF can be expressed as:

$$p(x_k | z_{1:k}) \approx \sum_{k=1}^N \omega_k^i \delta(x_k - x_k^i) \quad (17)$$

$$\omega_k^i \propto \omega_{k-1}^i \frac{p(z_k | x_k^i) p(x_k | x_{k-1}^i)}{q(x_k | x_{k-1}^i, z_k)} \quad (18)$$

where  $x_k^i$  is the estimated state value of particle  $i$  at the  $k^{th}$  step,  $\omega_k^i$  the estimated weight of particle  $i$  at the  $k^{th}$  step. The  $q(x_k | x_{k-1}^i, z_k)$  is an importance density.  $N$  is the number of particles, and  $\delta$  is the Dirac delta function. Below is the benchmark PF algorithm with sequential importance sampling (SIR) and resampling [1]:

The PF procedure:

- Step 1: initialise a set of particles  $\{(x_0^i, \omega_0^i): i=1, 2, \dots, N\}$  and some other parameters (process noise, measurement noise, etc.)
- Step 2: Draw  $x_k^i \sim q(x_k | x_{k-1}^i, z_k)$  and assign the particle a weight
- Step 3: Calculate and normalise weights
- Step 4: Resample  $\{x_k^i\}_{i=1}^N$  according to weight to obtain  $N$  random samples  $\{x_k^i\}_{i=1}^N$  with equal weights  $N^{-1}$
- Step 5: Estimate the voltage using the observation equation
- Step 6: Loop back to step 2 and repeat steps until the predicted time

In PF, the model coefficients  $\{a_1, a_2, a_3, a_4, a_5\}$  can be updated with new voltage data. For example, at  $t_l$ , we can use the model with updated parameters to predict the voltage in the future time  $t_\tau$ . We can obtain the RDT when the predicted voltage reaches the threshold

$\xi$ . Supposing the number of particles is  $N$ , then at time  $t_\tau$ , the predicted voltage of particle  $i$  can be expressed as:

$$E^i(t_\tau) = E'_0 - a_{1,i} e^{-\frac{a_{2,i}}{t_\tau}} - a_{3,i} e^{a_{4,i}t_\tau} + a_{5,i}t_\tau \quad (19)$$

The estimation of  $E(t_\tau)$  at time  $t_\tau$  is given by:

$$E(t_\tau) = \frac{1}{N} \sum_{i=1}^N E^i(t_\tau) \quad (20)$$

So, given the value of threshold  $\xi$ , the  $RDT_{t_l}^i$  at time  $t_l$  can be solved with the equation:

$$\begin{cases} E'_0 - a_{1,i} e^{-\frac{a_{2,i}}{t}} - a_{3,i} e^{a_{4,i}t} + a_{5,i}t = \xi \\ RDT_{t_l}^i = t - t_l \end{cases} \quad (21)$$

Here it's difficult to obtain the exact solution  $t$  in the above equation, so we adopt an approximate solution. To consider the evolution of the time sequence  $T = \{t_l + \Delta t, t_l + 2\Delta t, \dots, t_l + m\Delta t, \dots\}$  at regular intervals, the predicted voltage set  $E_{1:k} = \{E_i, i = 1, 2, \dots, m\}$  up to time  $m$  can be obtained with Eq. (16). We regard the first hitting time  $t$  whose voltage is greater than or equal to  $\xi$  as the solution of above equation. Thus, the estimation of RDT at prediction time  $t_l$  is given by:

$$t_{est} = \frac{1}{N} \sum_{i=1}^N RDT_{t_l}^i \quad (22)$$

To this point, the general procedures for predicting Lithium-ion Battery degradation with our method can be sketched as in Fig.7. To summarize, our new method has two phases, an off-line phase and an on-line phase. In the off-line phase, we apply PSO to identify the parameters  $\{a_1, a_2, a_3, a_4, a_5\}$ , to find all the parameter depletion trends, and to specify the relationship of age-related parameters  $\{a_1, a_4\}$  between discharge stages. In the on-line phase, using the PSO method, we obtain the initial parameters  $\{a_1, a_4, a_5\}$ , in which  $a_4 = m_1 a_1 + m_2$ . Then we apply PF to update all parameters for tracking the trend of battery discharging. Lastly, given the voltage threshold, RDT prediction is performed.

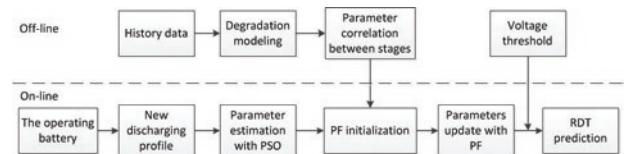


Fig. 7. A general procedure for degradation-based RDT prediction

## 5. A case study

### 5.1. Results

We take the case of RW3 as an example of RDT prediction using our method, here. The total number of reference discharge cycles in RW3 is 44. We chose three reference discharge cycles, 11, 22 and 32 to validate our method, as these three cycles have data for the entire battery life period, i.e., one fourth, two fourths, and three fourths of battery life. In addition, we chose a starting point for prediction in the

2000s, about one-third of one discharge cycle. The battery voltage threshold was 3.2V. RDT prediction results for RW3 cycles 11, 22 and 32 are shown in Fig. 8 (a)-(c). To express the uncertainty in our RDT predictions, we provide the probability density function (PDF) with 95% confidence bounds for the three discharge cycles. In Fig.8, due to the approximate nature of the empirical model, mentioned in Section 2, the prediction curves are not a good fit with the true curves in the last stage of the discharge cycle, especially later in the battery life cycle. However, the end of discharge (EOD) time of these four cycles is very close to the real EOD time. We present the prediction performance of the test battery RW3 in Table 2, including prediction error (PE), 95% confidence lower and upper bounds of RDT, and the root mean square error (RMSE). PE can be expressed as:

$$PE_{t_l}^r = \frac{|t_{est}^r - t_{true}^r|}{t_{true}^r + t_l} \quad (23)$$

where,  $PE_{t_l}^r$  denotes the prediction error at predicted time  $t_l$  for cycle  $r$ ;  $t_{est}^r$  is the estimation of RDT;  $t_{true}^r$  is the true RDT. Meanwhile, the RDT prediction results of RW4 and RW5 are shown in Figs. 9 and 10, for one fourth, two fourths, and three fourths of battery life. Table 3 displays the prediction performance for the test battery RW4; Table 4 shows that for RW5.

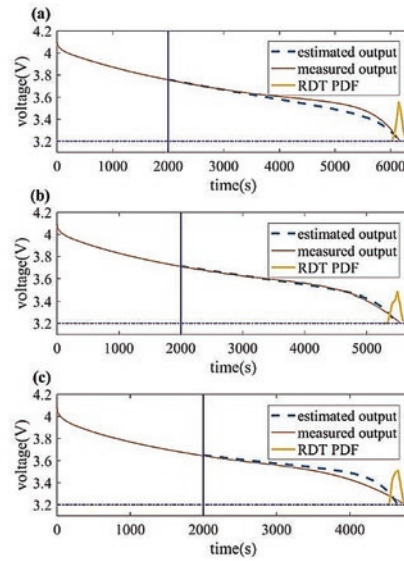


Fig. 8. RDT prediction in RW3 results for the (a) 11<sup>th</sup> cycle, (b) 22<sup>nd</sup> cycle, (c) 32<sup>nd</sup> cycle, at the 2000s

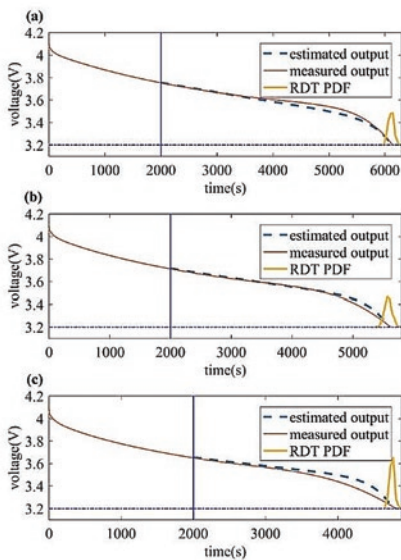


Fig. 10. RDT prediction in RW5 results for the (a) 10<sup>th</sup> cycle, (b) 21<sup>st</sup> cycle, (c) 32<sup>nd</sup> cycle, at the 2000s

### 5.2. Comparison and analysis

To show that our proposed method is appropriate for all battery life cycles, we provide PEs at the following percentiles of RW3 battery life cycle, 10%, 20%, and 90%. We also compared the proposed method with a benchmark PF-based method. The mean PEs for our proposed method and the PF method are given in Fig.11; the PEs for our method are far smaller than those for the PF method. Additionally, the PEs for the PF method increase over time. These results demonstrate that our proposed method, using PSO-PF and the linear relationship between age-related parameters, outperforms the PF method. Moreover, the established correlation between discharge stages can decrease future uncertainty and improve RDT accuracy.

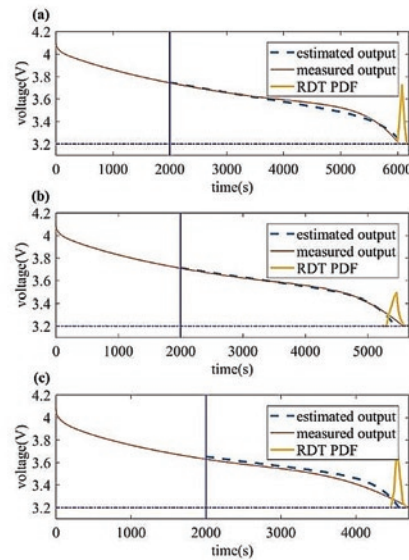


Fig. 9. RDT prediction in RW4 results for the (a) 10<sup>th</sup> cycle, (b) 19<sup>th</sup> cycle, (c) 29<sup>th</sup> cycle, at the 2000s

The RDT prediction results for RW3 cycles, 11, 21 and 32 using the benchmark PF-based method are shown in Fig.12 (a)-(c). Compared with our method, the benchmark PF-based method performs significantly worse in early prediction. Fig.13 shows the estimated values of parameters  $\{a_1, a_4\}$ . As expected, the estimated values of  $a_1$  are relatively close to true values for both methods. However, our method of estimating parameter  $a_4$  performs better than the benchmark PF-based method, so we get more accurate RDT predictions. This is mainly because using age-related parameters relationship data between the first and the third stages in the discharge estimation process, enables us to derive more accurate parameters with limited data. As mentioned earlier, an individual discharge process includes three separate stages, i.e. the self-discharge stage, the mass transfer

Table 2. Prediction performance for RW3

Cycle(r)	True RDT	Predicted RDT	PE	[lower, upper]	RMSE
11	4134	4130	0.07%	[4110,4250]	0.01978
22	3625	3600	0.45%	[3470,3780]	0.01414
32	2805	2767	0.80%	[2690,2860]	0.03241

Table 3. Prediction performance for RW4

Cycle(r)	True RDT	Predicted RDT	PE	[lower, upper]	RMSE
10	4165	4174	0.15%	[4040,4320]	0.02988
19	3547	3491	1.02%	[3360,3700]	0.01064
29	2758	2660	2.06%	[2570,2750]	0.03313

Table 4. Prediction performance for RW5

Cycle(r)	True RDT	Predicted RDT	PE	[lower, upper]	RMSE
10	4031	4102	1.16%	[4040,4150]	0.01802
21	3564	3447	2.11%	[3340,3660]	0.01770
32	2705	2577	2.71%	[2510,2680]	0.03834

stage, and the reactant depletion stage. When information related to the third stage is not available for early prediction, we can't obtain accurate parameters. However, once the proposed method utilizes the data related to the quantitative relationship between age-related parameters in the first and third stages, model parameters in the early stage of discharge can be revised to reflect the future model parameters. Thus, our proposed method predicts RDT more accurately than the benchmark PF-based prediction method, regardless of the degradation period of the battery.

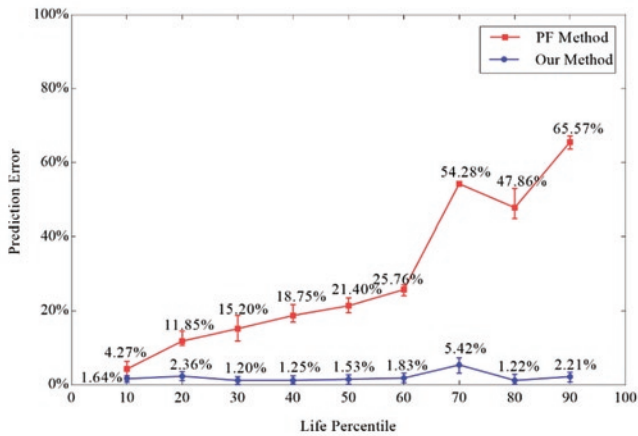


Fig. 11. Mean PEs for our method and the PF method

### 6. Conclusion

This paper presents a novel method for early prediction of RDT in Lithium-ion batteries that incorporates future information about battery discharge process. Differing from previous methods, our method doesn't start by analyzing the entire degradation process of a battery. We obtain information about future battery condition by decomposing the discharge model into three stages, based on levels of voltage loss. Using this structure, we specify the correlation between the model parameters at the first and last stages of discharge and use PSO and PF methods to update parameters. The values of model pa-

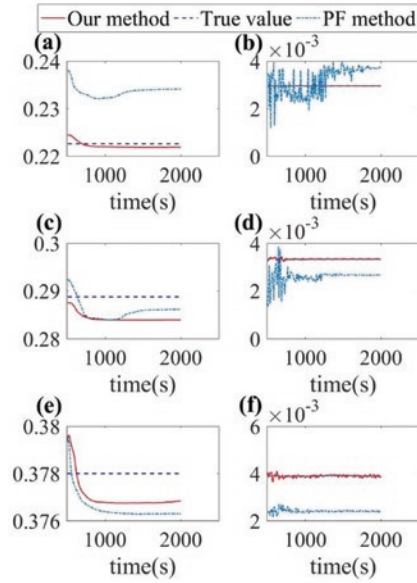


Fig. 12. RDT prediction results for RW3 with the PF-based method for the (a) 10<sup>th</sup> cycle, (b) 21<sup>st</sup> cycle, (c) 32<sup>nd</sup> cycle, at the 2000s

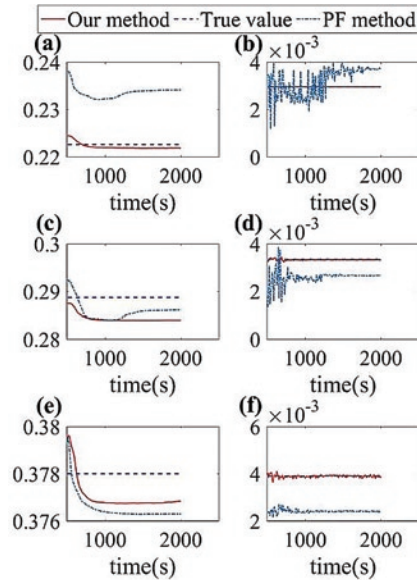


Fig. 13. Comparison between our method and the PF method re updating parameters  $\{a_1, a_4\}$  for the (a-b) 10<sup>th</sup> cycle, (c-d) 21<sup>st</sup> cycle, and (e-f) 32<sup>nd</sup> cycle. On the left: the estimated value of  $a_1$ . On the right: the estimated value of  $a_4$

rameters in the early stage of discharge can be revised to reflect the values of the future model parameters. With this method, we obtain a precise early RDT prediction parameters regardless of the degradation period of the battery, if the cut-off voltage is given. A study using real data showed that our proposed method, which considers correlation between discharge stages, performs better than the standard PF method. By sharing knowledge about model parameters between discharge stages, we obtain more accurate parameters from new observations, and thus make more accurate early RDT predictions.

However, there remains considerable room for improvement. In this paper, our method is tested under a fixed load. In many cases, however, the battery has a variable load profile. The variable loading condition will be investigated in the future. We believe that our proposed method can deal with this situation. In fact, we have already

figured out that, as long as an appropriate battery model is selected, our proposed method is completely capable of accommodating the variable loading situations. According to our investigation, the empirical model [21] can be used to describe the voltage degradation under the variable loading situation. There are three major causes for voltage drop in one discharge cycle, i.e. self-discharge, cell reactant depletion, and increasing internal resistance. Our model also uses real physical properties of Lithium-ion batteries and the parameters in our model

describe real physical characteristics of batteries. Battery characteristics will not change much under a fluctuating load. So, it will exist similar correlation between stages, and extracted correlation between parameters in the stages will still be useful. Then we can employ it in the PSO and PF methods to update parameters under a variable load. Our proposed method will be developed to be applicable under variable loading profiles in future.

## References

1. Arulampalam M S, Maskell S, Gordon N, Clapp T. A tutorial on particle filters for online nonlinear/non-Gaussian Bayesian tracking. *IEEE Transactions on Signal Processing* 2002; 50(2):174-188, <https://doi.org/10.1109/78.978374>.
2. Bole B, Kulkarni C S, Daigle M. Adaptation of an electrochemistry-based Li-ion battery model to account for deterioration observed under randomized use, Annual Conference of the Prognostics and Health Management Society, Fort Worth 2014.
3. Daigle M, Kulkarni C S. Electrochemistry-based battery modeling for prognostics, Annual Conference of the Prognostics and Health Management Society, New Orleans 2013.
4. Dalal M, Ma J, He D. Lithium-ion battery life prognostic health management system using particle filtering framework. *Journal of Risk & Reliability* 2015; 225 (1): 81-90.
5. Dong G, Wei J, Chen Z, Sun H, Yu X. Remaining dischargeable time prediction for lithium-ion batteries using unscented Kalman filter. *Journal of Power Sources* 2017; 364: 316-327, <https://doi.org/10.1016/j.jpowsour.2017.08.040>.
6. He Y, Liu X T, Zhang C B, Chen Z H. A new model for State-of-Charge (SOC) estimation for high-power Li-ion batteries. *Applied Energy* 2013; 101(1): 808-814, <https://doi.org/10.1016/j.apenergy.2012.08.031>.
7. Hu C, Jain G, Tamirisa P, Gorka T. Method for estimating capacity and predicting remaining useful life of lithium-ion battery. *Applied Energy* 2014; 126:182-189, <https://doi.org/10.1016/j.apenergy.2014.03.086>.
8. Hu C, Jain G, Zhang P, Schmidt C, Gomadam P, Gorka T. Data-driven method based on particle swarm optimization and k-nearest neighbor regression for estimating capacity of lithium-ion battery. *Applied Energy* 2014; 129:49-55, <https://doi.org/10.1016/j.apenergy.2014.04.077>.
9. Kasprzyk L. Modelling and analysis of dynamic states of the lead-acid batteries in electric vehicles. *Eksplatacja i Niezawodność – Maintenance and Reliability* 2017; 19(2): 229-236, <https://doi.org/10.17531/ein.2017.2.10>.
10. Kennedy J, Eberhart R. Particle swarm optimization, Proceedings of IEEE International Conference on Neural Networks, Perth 1995; 4: 1942-1948, <https://doi.org/10.1109/ICNN.1995.488968>.
11. Li K, Wei F, Tseng K J, Soong B H. A practical lithium-ion battery model for state of energy and voltage responses prediction incorporating temperature and ageing effects. *IEEE Transactions on Industrial Electronics* 2017;99:1-1.
12. Li Z, Huang J, Liaw B Y, Zhang J. On state-of-charge determination for lithium-ion batteries. *Journal of Power Sources* 2017; 348: 281-301, <https://doi.org/10.1016/j.jpowsour.2017.03.001>.
13. Liu J, Wang W, Ma F, Yang Y B, Yang C S. A data-model-fusion prognostic framework for dynamic system state forecasting. *Engineering Applications of Artificial Intelligence* 2012; 25(4): 814-823, <https://doi.org/10.1016/j.engappai.2012.02.015>.
14. Lu L, Han X, Li J, Hua J, Ouyang M. A review on the key issues for lithium-ion battery management in electric vehicles. *Journal of Power Sources* 2013; 226 (3): 272-288, <https://doi.org/10.1016/j.jpowsour.2012.10.060>.
15. Miao Q, Xie L, Cui H, Liang W, Pecht M. Remaining useful life prediction of lithium-ion battery with unscented particle filter technique. *Microelectronics Reliability* 2013; 53 (6): 805-810, <https://doi.org/10.1016/j.microrel.2012.12.004>.
16. Orchard M E, Cerda M, Olivares B, Silva J F. Sequential Monte Carlo methods for discharge time prognosis in lithium-ion batteries. *International Journal of Prognostics & Health Management* 2012; 3(2):1-12.
17. Pattipati B, Sankavaram C, Pattipati K. System identification and estimation framework for pivotal automotive battery management system characteristics. *IEEE Transactions on Systems Man & Cybernetics Part C* 2011; 41(6): 869-884, <https://doi.org/10.1109/TSMCC.2010.2089979>.
18. Pola D A, Navarrete H F, Orchard M E, Rabié R S, Cerda M A, Olivares B E, Silva J F, Espinoza P A, Pérez A. Particle-filtering-based discharge time prognosis for lithium-ion batteries with a statistical characterization of use profiles. *IEEE Transactions on Reliability* 2015; 64(2): 710-720, <https://doi.org/10.1109/TR.2014.2385069>.
19. Rahman M A, Anwar S, Izadian A. Electrochemical model parameter identification of a lithium-ion battery using particle swarm optimization method. *Journal of Power Sources* 2016; 307: 86-97, <https://doi.org/10.1016/j.jpowsour.2015.12.083>.
20. Saha B, Goebel K. Modeling Li-ion battery capacity depletion in a particle filtering framework, Annual Conference of the Prognostics and Health Management Society, San Diego 2009.
21. Saha B, Koshimoto E, Hogge E F, Strom T H, Hill B L, Goebel K. Predicting Battery Life for Electric UAVs, 2011 Infotech@Aerospace Conference, St. Louis 2011.
22. Saha B, Koshimoto E, Quach C C, Hogge E F, Strom T H, Hill B L, Vazquez S L, Goebel K. Battery health management system for electric UAVs, 2011 IEEE Aerospace Conference, Big Sky 2011; 1-9, <https://doi.org/10.1109/AERO.2011.5747587>.
23. Sbarufatti C, Corbetta M, Giglio M, Cadini F. Adaptive prognosis of lithium-ion batteries based on the combination of particle filters and radial basis function neural networks. *Journal of Power Sources* 2017; 344: 128-140, <https://doi.org/10.1016/j.jpowsour.2017.01.105>.
24. Schwaab M, Jr E C B, Monteiro J L, Pinto J C. Nonlinear parameter estimation through particle swarm optimization. *Chemical Engineering Science* 2008; 63(6): 1542-1552, <https://doi.org/10.1016/j.ces.2007.11.024>.
25. Virkar A V. A model for degradation of electrochemical devices based on linear non-equilibrium thermodynamics and its application to lithium ion batteries. *Journal of Power Sources* 2011; 196(14): 5970-5984, <https://doi.org/10.1016/j.jpowsour.2011.03.005>.



26. Walker E, Rayman S, White R E. Comparison of a particle filter and other state estimation methods for prognostics of lithium-ion batteries. *Journal of Power Sources* 2015; 287(4): 1-12, <https://doi.org/10.1016/j.jpowsour.2015.04.020>.
27. Wang D, Miao Q, Pecht M, Pecht Michael. Prognostics of lithium-ion batteries based on relevance vectors and a conditional three-parameter capacity degradation model. *Journal of Power Sources* 2013; 239(10): 253-264, <https://doi.org/10.1016/j.jpowsour.2013.03.129>.
28. Wang Y, Chen Z, Zhang C. On-line remaining energy prediction: A case study in embedded battery management system. *Applied Energy* 2016; 194: 688-695, <https://doi.org/10.1016/j.apenergy.2016.05.081>.
29. Xu X, Chen N. A state-space-based prognostics model for lithium-ion battery degradation. *Reliability Engineering & System Safety* 2017; 159: 47-57, <https://doi.org/10.1016/j.res.2016.10.026>.
30. Xu X, Li Z, Chen N. A hierarchical model for lithium-ion battery degradation prediction. *IEEE Transactions on Reliability* 2016; 65(1): 310-325, <https://doi.org/10.1109/TR.2015.2451074>.
31. Yu J, Liang S, Tang D, Liu H. Remaining discharge time prognostics of lithium-ion batteries using Dirichlet process mixture model and particle filtering method. *IEEE Transactions on Instrumentation & Measurement* 2017; PP(99):1-12.
32. Zhang X, Wang Y, Liu C, Chen Z H. A novel approach of remaining discharge energy prediction for large format lithium-ion battery pack. *Journal of Power Sources* 2017; 343: 216-225, <https://doi.org/10.1016/j.jpowsour.2017.01.054>.
33. Zheng X, Fang H. An integrated unscented Kalman filter and relevance vector regression approach for lithium-ion battery remaining useful life and short-term capacity prediction. *Reliability Engineering & System Safety* 2015; 144: 74-82, <https://doi.org/10.1016/j.res.2015.07.013>.
34. Zio E, Peloni G. Particle filtering prognostic estimation of the remaining useful life of nonlinear components. *Reliability Engineering & System Safety* 2011; 96(3): 403-409, <https://doi.org/10.1016/j.res.2010.08.009>.

---

**Jinsong YU**

School of Automation Science and Electrical Engineering  
Beihang University  
No.37 Xueyuan Road, Haidian District, Beijing 100191, China  
Collaborative Innovation Center of Advanced Aero-Engine, Beijing 100191, China

**Jie YANG****Diyin TANG**

School of Automation Science and Electrical Engineering  
Beihang University  
No.37 Xueyuan Road, Haidian District, Beijing 100191, China

**Jing DAI**

China Academy of Launch Vehicle Technology R&D center  
NO.1 Nan Da Hong Men Road, Feng Tai District, Beijing 100191, China

Emails: yujs@buaa.edu.cn, megan\_yj@buaa.edu.cn, tangdiyin@buaa.edu.cn,  
buaadaij@126.com

---